

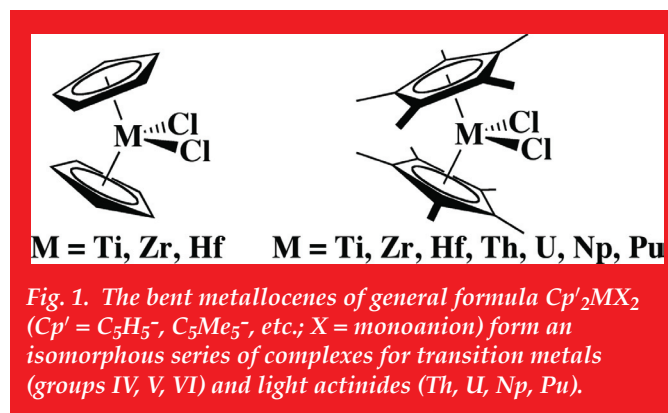
Covalency Trends in Group IV Metallocene Dichlorides: Chlorine K-edge X-ray Absorption Spectroscopy and Time Dependent-density Functional Theory

Ping Yang, Enrique R. Batista, P. Jeffrey Hay, Richard L. Martin, T-12; Stosh A. Kozimor, Carol J. Burns, C-NR; Kevin S. Boland, Laura E. Wolfsberg, C-IIAC; David L. Clark, Daniel E. Schwarz, ADSMS; Steven D. Conradson, Juan S. Lezama, MST-8; Marianne P. Wilkerson, C-ADI; Christin N. Christensen, New Mexico State Univ.

The bent metallocenes of general formula $\text{Cp}'_2\text{MX}_2$ ($\text{Cp}' = \text{C}_5\text{H}_5^-, \text{C}_5\text{Me}_5^-, \text{etc.}; \text{X} = \text{monoanion}$) form an isomorphous series of complexes for transition metals (groups IV, V, VI) and light actinides (Th, U, Np, Pu), and are among the most extensively utilized molecular systems in organometallic research. Theoretical and spectroscopic studies of metallocenes indicate that variations in orbital character and metal d - and f -covalency are connected with differences in chemical reactivity. Of the experimental approaches to determine covalency, ligand K-edge x-ray absorption spectroscopy (XAS) has emerged as a powerful measure of the amount of ligand orbital mixing with metal-based orbitals. On the low-energy side of the ligand K-edge are bound state transitions of ligand $1s$ electrons into metal-based orbitals that contain ligand p character due to covalent mixing. The intensity of these pre-edge features provides a direct experimental measure of covalency.

Since the $\text{Cp}'_2\text{MCl}_2$ compounds form an isomorphous series for transition metals and light actinides (Fig. 1), they are well-suited for a ligand K-edge XAS study to compare relative changes in orbital mixing between a common Cl^- ligand and $3d$, $4d$, $5d$, and $6d/5f$ orbitals in metal-ligand bonding. Moreover, their electronic structure is well understood, and the Cl K-edge XAS of the first member of this series, Cp_2TiCl_2 ($\text{Cp} = \text{C}_5\text{H}_5^-$), has been recently analyzed by both experiment and theory, thereby providing a standard for comparison with heavier congeners.

For a more detailed understanding of M-Cl bonding interactions we employed electronic structure calculations on Cp_2MCl_2 complexes using B3LYP hybrid density functional theory (DFT) in the *Gaussian 03* code. The Stuttgart 97 relativistic effective core potential and associated basis sets (minus the most diffuse function) were used for Ti, Zr, and Hf, and the 6-31 G* basis sets for C and H.



The first level of theory assumes that the transition amplitudes are directly proportional to the % Cl p character of the virtual orbitals. A more rigorous level of theory involves a linear response theory (TD-DFT)

calculation, where the probability amplitudes were extracted from the transition dipole moments between the calculated excited states and the ground states. The excitations originating from all the intermediate states between the Cl $1s$ and the highest occupied molecular orbital (HOMO) were not included so that only excitations from the core levels to virtual molecular orbitals (MOs) could be analyzed. This allows the virtual orbitals to mix among themselves to reflect the presence of the core hole in Cl. However, we do not include relaxations in the occupied orbitals associated with the core hole.

The electronic structure of bent metallocene dichlorides is well understood. The bent Cp_2M fragment is characterized by six M-Cp orbital interactions at lower energy, leaving three low-energy metal orbitals ($1a_1$, $1b_2$, and $2a_1$) and two higher-lying metal orbitals ($1b_1$, $2b_2$) available to form bonding interactions with the Cl ligands. While the first set of three orbitals is generally regarded as the most important for M-Cl bonding, all five are necessary to understand the XAS intensities. The five resulting M-Cl antibonding orbitals are shown in Fig. 2.

From ground state calculations, the total calculated % Cl $3p$ character for the metal-based orbitals is 20%, 18%, and 17%, Cp_2MCl_2 complexes ($\text{M} = \text{Ti, Zr, and Hf}$; **1**, **2**, and **3**, respectively), which agrees well with the experimental values. From the more rigorous TD-DFT calculations we were able to simulate the Cl K-edge XAS, and this is compared with experimental XAS in Fig. 3. The TD-DFT calculations reproduce the basic experimental features of peak intensity, peak area, and peak energies remarkably well, and provide additional confidence on spectral assignments. The calculated and experimental spectra for **1-3**, Fig. 3, show a decrease in amplitudes and increase in peak width for the second pre-edge feature. The increase in width stems from the larger splitting among the d virtual states, and the decrease in intensity to an overall reduction in oscillator strength.

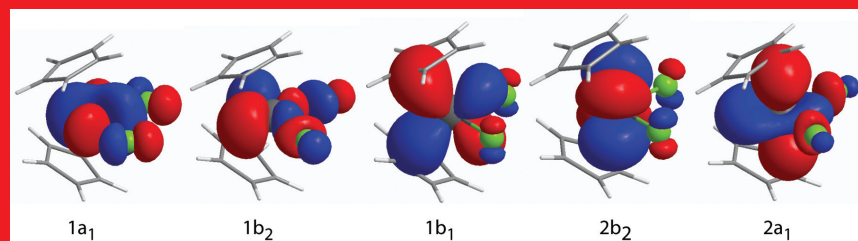


Fig. 2. Shape of five M-Cl antibonding orbitals in the electronic structures of bent metallocene dichlorides Cp_2MX_2 ($M = \text{Ti}, \text{Zr}, \text{Hf}$).

For all three compounds, our TD-DFT calculations suggest that the two lowest unoccupied orbitals are the $1a_1$ and $1b_2$ M-Cl anti-bonding orbitals. Hence, for **1-3** the first XAS pre-edge peak is attributed to a $\text{Cl } 1s \rightarrow 1a_1$ transition. While it is tempting to assign the second pre-edge peak to a $1s \rightarrow 1b_2$ transition, the calculations reveal that the $1b_2$ orbital is pushed sufficiently high in energy such that the manifold of four primarily metal nd molecular orbitals ($1b_2$, $1b_1$, $2b_2$, and $2a_1$) are closely grouped together, spanning only 0.6, 0.9, and 1.1 eV for **1-3**,

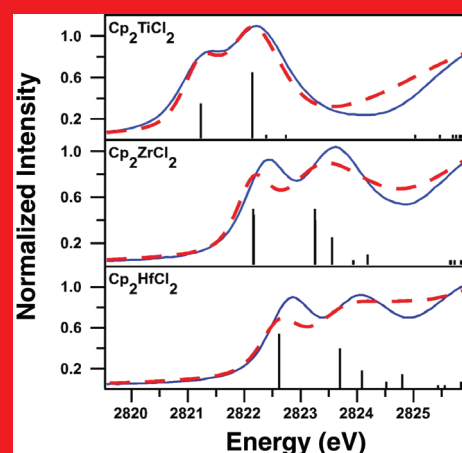


Fig. 3. The Cl K-edge experimental data (blue), the TD-DFT calculated spectrum (red dashes), and the TD-DFT calculated transitions (black bars) for polystyrene films of Cp_2MCl_2 ($M = \text{Ti}$ top, Zr middle, and Hf bottom; **1**, **2**, and **3**, respectively).

respectively. Depending on the metal ion, all four metal d orbital mix with the Cl $3p$ orbitals to varied extents with orbital mixing following the order $\text{Hf} > \text{Zr} > \text{Ti}$. For example, in **1** the $1s \rightarrow 1b_2$ transition contributes 87% to the total intensity of the second peak, while smaller contributions from the $1s \rightarrow 1b_1$, $2b_2$, and $2a_1$ transitions provide the additional 13%. In contrast, the amount of metal Cl $3p/\text{Hf } 5d$ mixing is more evenly distributed in **3** and the $1s \rightarrow 1b_2$ transition accounts for only 56% of the total intensity of the second peak. These calculations are consistent with the experimental spectra for **1-3**, which show decreased amplitudes and increased peak widths for the second pre-edge features.

Both theory and experiment indicate that the M-Cl bond for the $3d$ complex, **1**, is more covalent than the $5d$ analogue, **3**. Although the covalency in the Zr-Cl bond for **2** was experimentally indistinguishable from that of the Ti-Cl bond in **1**, the calculations suggest higher % Cl $3p$ character for **1** than for **2**. Since the percent of Cl $3p$ character in the $1a_1$ molecular orbital was calculated, as well as found experimentally, to be the same for all three complexes, the differences in total covalency for the M-Cl bonds are attributable to the degree of Cl $3p$ orbital mixing with the $1b_2$, $1b_1$, $2b_2$, and $2a_1$ manifold of metal d orbitals, which decreases from **1** to **3**. This finding is similar to the trends revealed by gas phase photoelectron spectroscopy of occupied orbitals in metallocene complexes reported by Marks and coworkers.

Theoretical and spectroscopic studies of metallocenes indicate that variations in orbital character and metal d-covalency are connected with differences in chemical reactivity. Our results demonstrate the utility of Cl K-edge XAS for quantitatively analyzing the covalent mixing in M-Cl bonds along the series of $3d$, $4d$, and $5d$ group IV complexes. Along this series, covalency decreases, and the % Cl character is concomitantly spread over a greater number of MOs as Z increases. These data also demonstrate that reliable intensity data can be obtained using polystyrene-encapsulated samples, which should allow us to extend these studies to the heavier actinide series where both $5f$ and $6d$ orbitals are expected to play a role in M-Cl bonding, and where transition assignments must rely on accurate theoretical calculations.

These studies have now been extended to the light actides, where evidence of covalency in the $5f$ orbitals has been observed. The degree of interaction is roughly half that observed in the transition metal benchmarks. Further experimental and theoretical studies should reveal a great deal about this fundamental issue in chemical bonding.

For further information contact Richard L. Martin at rlmartin@lanl.gov.

Funding Acknowledgments

- Department of Energy, Office of Science, Office of Basic Energy Sciences
- Frederick Reines Postdoctoral Fellowship
- Glenn T. Seaborg Institute